PROCEEDINGS OF SCIENCE

Analysis of the composition of TeV cosmic rays with HAWC

J.C. Arteaga-Velázquez[a,*] **for the HAWC Collaboration**

[a] *Instituto de Física y Matemáticas,*
Universidad Michoacana, Morelia, Michoacan, Mexico

E-mail: juan.arteaga@umich.mx

We present the results of an analysis of the composition and energy spectra of cosmic rays for energies between 10 TeV and 1 PeV. For the study, we made use of a large collection of air shower data detected with HAWC during five years of observation. The corresponding measurements on the lateral shower age and the primary energy of the events were analyzed using the Gold unfolding algorithm, which allowed us to separate the elemental spectra for three mass groups: H, He and heavy nuclei ($Z > 2$). For the reconstruction of the spectra, we used CORSIKA/QGSJET-II-04 simulations. The results confirm the presence of softenings at tens of TeV in the spectra of the light mass groups of cosmic rays and hardenings at around 100 TeV in these spectra. In addition, they also show an increment in the relative composition of heavy elements at high energies.

38th International Cosmic Ray Conference (ICRC2023)
26 July - 3 August, 2023
Nagoya, Japan

*Speaker

PoS(ICRC2023)299

1. Introduction

The origin, acceleration mechanism, composition and the details of the propagation of cosmic rays of high energies are not fully understood. Precision measurements on the primary energy, composition and arrival direction of cosmic rays and complementary information from the multi-messenger astronomy are needed in order to discard and build astrophysical models that can allow us to explain the observations on these extraterrestrial radiation. At TeV energies, HAWC is contributing in two fronts by looking for cosmic-ray sources with gamma-ray observations of the sky and by measuring the energy spectrum, anisotropies and composition of galactic cosmic rays.

HAWC is an air-shower array detector dedicated to the study of TeV cosmic-rays and gamma-rays. It is located at an elevation of 4100 m on a terrace of the Sierra Negra Volcano in the state of Puebla, Mexico [1]. For the detection of extensive air-showers, a compact array of 22000 m^2 that is composed of 300 water Cherenkov detectors is employed in HAWC. Each detector consists of a cylindrical tank (7.3m diameter and 4.5m high) made of steel, which is instrumented with four photomultipliers (PMT). The detector measures the arrival times of the shower particles and the deposited energy, which is converted to local charge by a dedicated calibration procedure. The reconstruction of the EAS is done off-line and provides, among other observables, the shower core, the zenith and azimuth of the shower axis, the lateral distribution function, i.e., the effective charge per PMT as a function of the radial distance, the shower age and the primary energy. The latter is estimated with a maximum likelihood procedure [2] which is based on a comparison of the LDF of the EAS event with the predictions of full EAS-detector simulations produced for cosmic-ray protons using QGSJET-II-04 [3]. The shower age is computed on an event-by-event basis from a fit to the LDF data with an NKG-like function using a χ^2 minimization procedure [4]. In this work, using the HAWC data for the shower age and the primary energy, we have investigated the composition of TeV cosmic rays. In particular, we have employed an unfolding procedure to separate the energy spectra for protons, helium nuclei and heavy primaries ($Z > 2$) in the energy interval from 10 TeV to 1 PeV. In the next sections we will describe the experimental data and the Monte Carlo (MC) simulations. Then, we will present the selection cuts and the analysis procedure. Next, we will show the findings of our research. Finally, we will discuss the results and present the conclusions.

2. Analysis method

The measured data consist of shower events collected between 2016 and 2020. The effective time of observation correspond to $T_{\text{eff}} = 4.7$ years. The selected data contain 37.5×10^9 EAS and include events that were successfully reconstructed, with zenith angles $\theta = [20°, 45°]$ and shower age $s = [1.0, 3.8]$, with more than 40 activated PMTs within a radius of 40 m from the EAS core, fraction of hit PMTs ≥ 0.2, more than 900 working PMTs, with a lateral amplitude smaller than $10^{2.6}$ and a reconstructed primary energy in the range $\log_{10}(E_{rec}/\text{GeV}) = [3.8, 6.5]$. The selection cuts were studied from MC simulations and were applied to MC and measured data to reduce the effect of systematic errors in our results. We avoided to use vertical showers, because we observed that above $\log_{10}(E_{rec}/\text{GeV}) = 5.5$ the systematic uncertainties of the spectra increase exponentially. According to the predictions of the MC simulations, we found that for energies $E_{rec} > 10$ TeV, the

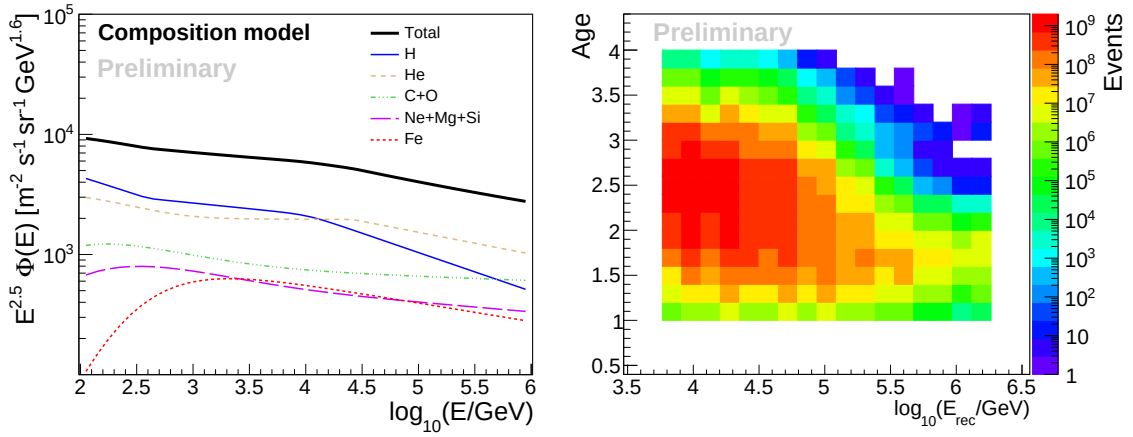

Figure 1: Left: The nominal composition model of cosmic rays employed in the present analysis. Right: The measured shower age vs reconstructed energy distribution after applying selection cuts.

shower core and angular resolutions of the instrument are 20 m and 0.7°, respectively, while the energy resolution is $\sigma \log_{10}(E_{rec}/\mathrm{GeV}) < 0.4$.

To build our MC simulations, we used CORSIKA v7.40 [5] and the high-energy hadronic interaction model QGSJET-II-04. With this software, we generated EAS for H, He, C, O, Ne, Mg, Si and Fe primaries, using $\theta < 65°$ and primary energies from 5 GeV to 10 PeV, as well as energy spectra proportional to E^{-2}. We weighted the MC simulations to reproduce the intensities of a cosmic-ray composition model (see Fig. 1, left) that was derived by fitting broken power-law functions to data from ATIC-2 [6], CREAM I-II [7, 8], PAMELA [9, 10], AMS-2 [11–14], NUCLEON [15], CALET [16, 18, 19], DAMPE [20, 21] and KASCADE [22]. We simulated the interaction of the particle showers with the detector using a code based on GEANT4 [23]. The simulated data was reconstructed with the same algorithm employed for the measured data.

To start with the analysis, we obtained the bidimensional distribution, $n(s, \log_{10} E_{rec})$, of the lateral shower age against the reconstructed primary energy for the measured data (see Fig. 1, right). The energy spectra of the elemental mass groups of cosmic rays and the measured distribution are related in the following way:

$$n(s, \log_{10} E_{rec}) = T_{\mathrm{eff}}\, \Delta\Omega \sum_{j=1} \sum_{E} P_j(s, \log_{10} E_{rec} | \log_{10} E)\, A_{\mathrm{eff},j}(E)\, \Phi_j(E)\, \Delta E, \qquad (1)$$

where j runs over each mass group and E over each true energy bin. Here $\Phi_j(E)$ represents the energy spectrum of a given primary cosmic ray, $P_j(s, \log_{10} E_{rec} | \log_{10} E)$ is the response matrix, which give us the probability that a cosmic-ray event of type j and energy E that is detected and selected in HAWC is reconstructed with energy E_{rec} and shower age s, $\Delta\Omega$ and T_{eff} are the solid angle interval and effective time of observation, respectively, while $A_{\mathrm{eff},j}(E)$ is the effective area for the j mass group. We have considered three mass groups for the analysis, in particular, H, He and heavy nuclei ($Z > 2$).

To solve Eq. (1) for $\Phi_j(E)$, we have applied the Gold's unfolding algorithm [22, 24]. The procedure requires the calculation of the effective area and the response matrix. We compute them using our MC simulations and our nominal composition model. As the procedure is iterative we need an initial guess for the energy spectra. In this case, we considered the intensities of our

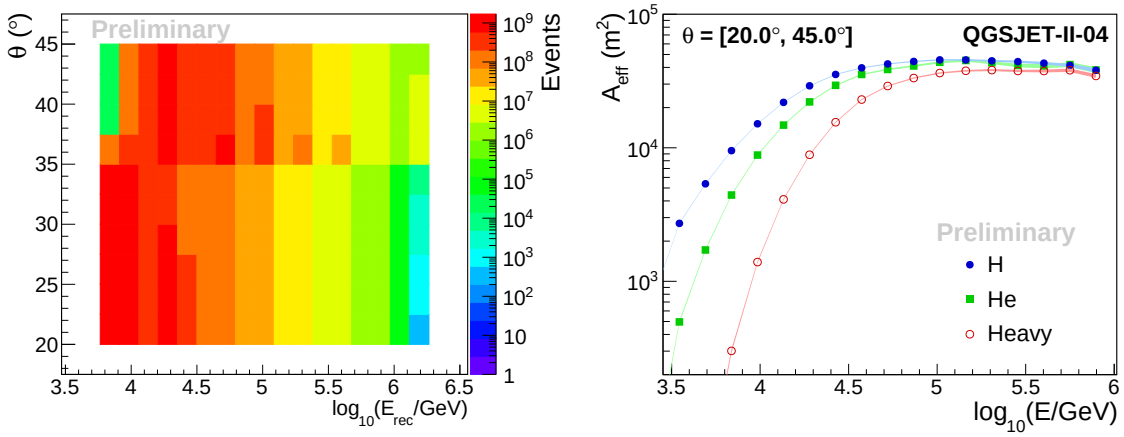

Figure 2: Left: The measured distribution for θ vs E_{rec} after using selection cuts. Right: The effective area of HAWC for H, He and heavy primaries estimated with MC simulations and our composition model.

cosmic-ray composition model. As the iteration depth increases, the χ^2 between $n(s, \log_{10} E_{rec})$ and the forwardfolded solution decreases. However, large iterations depths does not imply to have the best solution. We observe that for a large number of iterations, the χ^2 between the measured and the forwardfolded θ versus E_{rec} frequency distribution grows. Since this distribution also keep information about the composition of cosmic rays, to find the unfolded solution, we added as a further physical criterion to minimize the χ^2 for the $n(\theta, E_{rec})$ distribution. As a smoothing procedure we fitted the intermediate spectra with a broken power law. We employed the MINUIT [25] version of ROOT [26] for the unfolding procedure.

3. Results

The energy spectra for the H, He and heavy mass groups as obtained in our analysis are presented in Fig. 3, left. The total energy spectrum is also shown in this plot. On the other hand, the unfolded spectrum for H+He is compared with the solution for H and He primaries in Fig. 3, right. In each plot, we displayed the statistical and systematic uncertainties. The total statistical errors ($< 6\%$) receive contributions from the limited size of the MC simulations and the data sample, both of them were added in quadrature. On the other hand, for the calculation of the total systematic errors we evaluated the influence of the late-light effect, the charge resolution and the efficiency of the PMTs as well as the configuration of the experiment [4], the uncertainties due to the priors (using the spectra from the Polygonato [27] and the GSF [28] composition models), the unfolding method (using the Bayesian unfolding procedure [29]), the effective area, the composition model (employing the Polygonato, the GSF, the H3a [30] models and the uncertainties in the parameters of our nominal model) and the influence of the high-energy hadronic interaction model (using EPOS-LHC [31]). The individual contributions are added in quadrature to obtain the total systematic error ($< 42\%$), which is dominated by the uncertainties in the PMT modeling ($< 40\%$). The main effect of the systematic errors is to modify the relative cosmic-ray abundance. We do not observe an important effect on the shape of the spectra due to the systematic uncertainties.

From Fig. 3, we see that the unfolded spectra of the light and heavy mass groups are not featureless, all of them exhibit individual cuts. Besides, the energy spectra of the light nuclei show

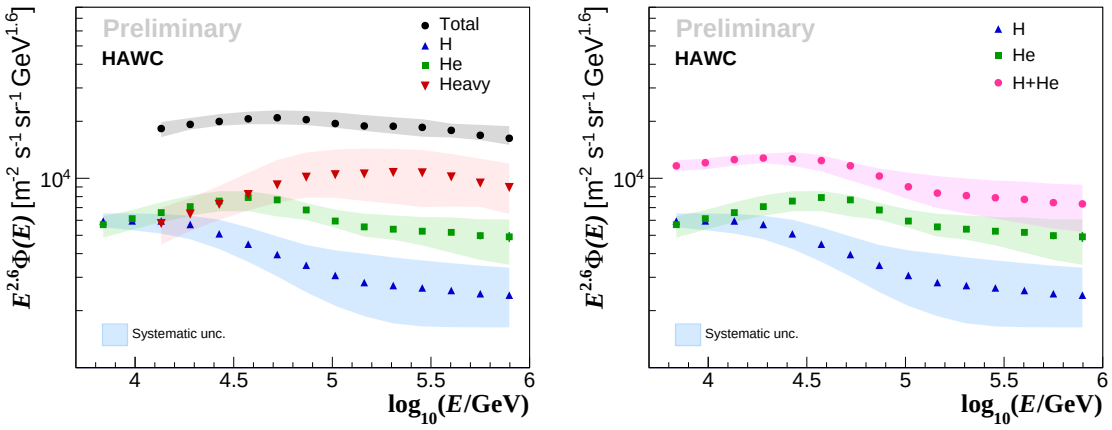

Figure 3: Left: The energy spectra for H (blue upward triangles), He (green squares) and heavy cosmic-ray nuclei (red downward triangles) obtained from the unfolding analysis with HAWC data. The all-particle energy spectrum , i.e., the sum of the individual spectra for H, He and heavy primaries, is plotted with black circles. Right: The energy spectrum of H+He nuclei (pink circles) in comparison with the spectra for H and He. Error bands represent systematic uncertainties and the error bars, statistical errors.

some hardenings. We have investigated the location of these structures by fitting the spectra with the broken power-law formula

$$\Phi(E) = \Phi_0 \, E^{\gamma_0} \left[1 + \left(\frac{E}{E_0}\right)^{\varepsilon_0}\right]^{(\gamma_1-\gamma_0)/\varepsilon_0} \left[1 + \left(\frac{E}{E_1}\right)^{\varepsilon_1}\right]^{(\gamma_2-\gamma_1)/\varepsilon_1}, \tag{2}$$

which has two breaks, one (E_0) at low energies and another one (E_1) at higher energies. In the above expression, Φ_0 is a normalization parameter, γ_i and γ_{i+1} are the spectral indexes of the function before and after the break at the energy E_i, with $i = 0, 1$, while ε_i is a parameter that describes the degree of smoothing of the feature. For our fits, we fixed ε_0 to 5 for the spectra of H and He primaries, 3 for the intensity of H+He nuclei and 10 for the spectrum of heavy elements. The results of the fits are presented in Fig. 4 and table 1. From this table, we observe that the cuts in the energy spectra of light elemental nuclei appears at tens of TeV, while the hardenings are located at approximately hundred TeV. On the other hand, we also see that the spectrum for the heavy component of cosmic rays has two softenings, one at 65 TeV and another one close to 323 TeV. By applying a statistical analysis based on the test statistics $\Delta\chi^2$, we found that the broken power law with two breaks is preferred by the data with more than 3σ of significance over the scenario with a single power-law.

From Fig. 3, left, we observe that the relative abundance of the light to heavy primaries decreases at high energies. In addition, we also see that the bump in the all-particle energy spectrum around tens of TeV is due to the existence of softenings in the spectra of the light and heavy mass groups. In the same way, from Fig. 3, right, we can say that the cut reported at tens of TeV for the spectrum of H+He nuclei is due to the superposition of breaks in the individual spectra of protons and helium primaries.

In Fig. 5, we compare our unfolded spectra with measurements of other experiments on TeV cosmic rays. From this plot, we confirm the softening observed by DAMPE [20] and CALET [32] in the spectrum of protons and the break of the spectrum for He reported by the DAMPE detector

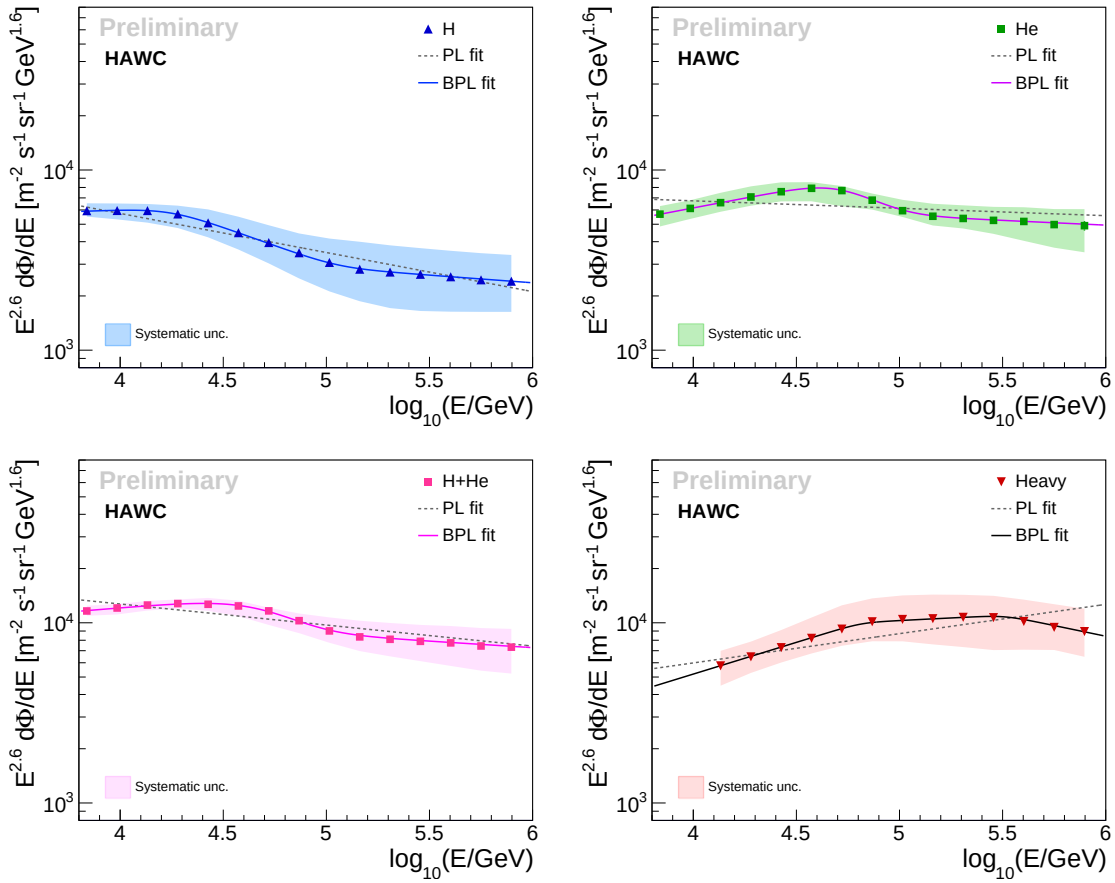

Figure 4: Fits to the unfolded energy spectra with the broken power law (BPL) of eq. (2), using the χ^2 minimization procedure and the statistical covariance matrix of the data. The dotted line is the result of the fit with a power law (PL) expression.

[21]. Furthermore, we also observe the cut previously measured by DAMPE [33] and HAWC [34] for the intensity of H+He primaries. We also see an overlapping of our measurements for protons with the data from direct experiments. We must point out that the HAWC measurements for He and H+He nuclei are in agreement with data from ATIC-02 [6] at around 10 TeV, but above other experimental data up to $\sim$ 100 TeV. We should mention that at high energies, above 126 TeV, the spectrum measured by HAWC for H+He primaries is in agreement with DAMPE [33] and ARGO-YBJ within systematic uncertainties [35]. Note that for the 10 – 100 TeV energy range, the HAWC measurements for the heavy component of cosmic rays agrees with data from ATIC-02 [6],

Mass group	E_0 (TeV)	E_1 (TeV)	γ_0	$\Delta\gamma_0 = \gamma_1 - \gamma_0$	$\Delta\gamma_1 = \gamma_2 - \gamma_1$
H	17.4 ± 0.6	$113.5^{+7.4}_{-7.0}$	-2.56 ± 0.01	-0.46 ± 0.01	0.33 ± 0.03
He	49.5 ± 1.3	$104.2^{+2.2}_{-2.1}$	-2.382 ± 0.004	-0.82 ± 0.03	0.55 ± 0.03
H+He	$51.2^{+3.8}_{-3.6}$	$90.3^{+9.3}_{-8.4}$	-2.506 ± 0.002	-0.79 ± 0.15	0.56 ± 0.16
Heavy	65.1 ± 1.3	$323.1^{+22.7}_{-21.2}$	-2.25 ± 0.01	-0.30 ± 0.01	-0.29 ± 0.02

Table 1: Results of the fits with Eq. (1) to the unfolded energy spectra of Fig. 3.

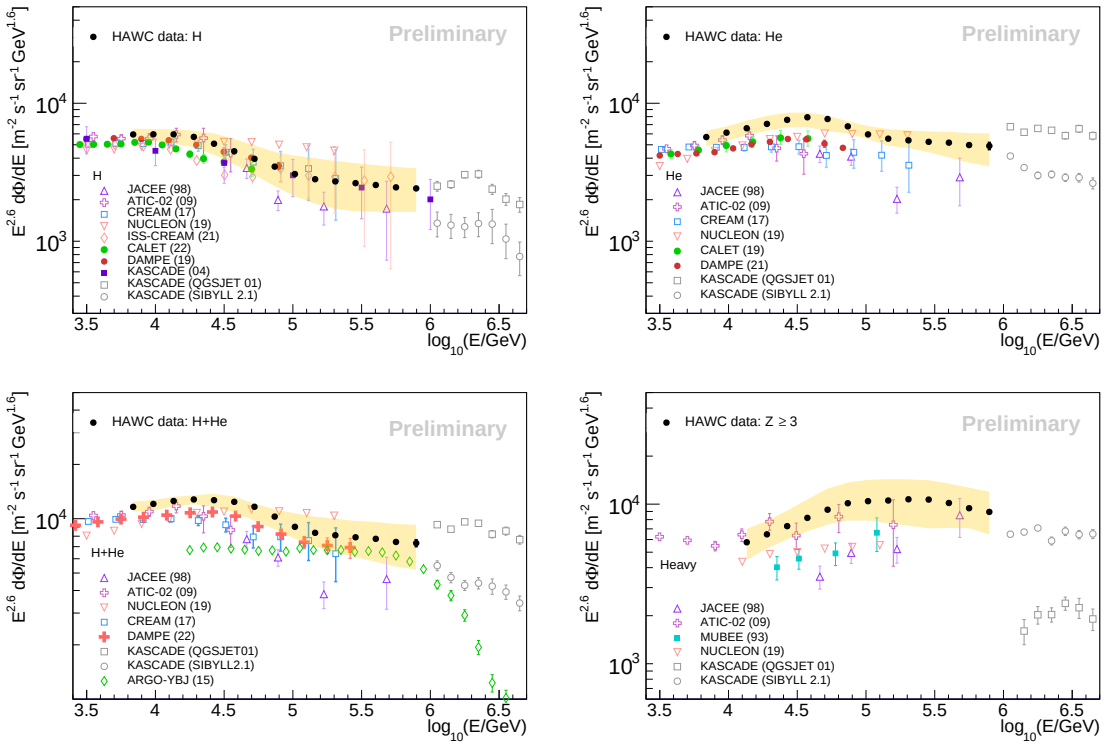

Figure 5: Comparisons of HAWC results with data from different experiments: ATIC-02 [6], NUCLEON [15] , DAMPE [20, 21], KASCADE [22], ARGO-YBJ [35], JACEE [36], MUBEE [37] and CREAM [38] and ISS-CREAM [39].

although it is above the measurements from NUCLEON [15], JACEE [36] and MUBEE [37]. In addition, we found that the intensity for the light elemental nuclei at around 1 PeV measured by HAWC is of the same order of magnitude than the corresponding one from KASCADE at around the same energy [22]. Finally, at around 1 PeV, the HAWC spectrum for the heavy component seems to be larger than that measured by KASCADE [22].

4. Conclusions

Using unfolding techniques, we have obtained the energy spectra for H, He and heavy cosmic-ray nuclei in the energy interval from 10 TeV to 1 PeV from EAS data on the lateral shower age and the estimated primary energy. Our results confirm the existence of cuts at tens of TeV for the spectra of H, He and H+He and also show the presence of a cut in the spectrum for the heavy mass group in the same energy range. On the other hand, at around 100 TeV energies, our measurements on the spectra of light elemental nuclei reveal the existence of new features, i.e. hardenings. We also found an additional softening in the spectrum of the heavy component of cosmic rays at energies of around $323.1^{+22.7}_{-21.2}$ TeV. We have estimated that the broken power-law hypothesis with two breaks is in better agreement with the data than the power-law scenario with at least 3σ of significance.

Acknowledgments. We acknowledge the support from: the US National Science Foundation (NSF); the US Department of Energy Office of High-Energy Physics; the Laboratory Directed Research and Development (LDRD) program of Los Alamos National

Laboratory; Consejo Nacional de Ciencia y Tecnología (CONACyT), México, grants 271051, 232656, 260378, 179588, 254964, 258865, 243290, 132197, A1-S-46288, A1-S-22784, cátedras 873, 1563, 341, 323, Red HAWC, México; DGAPA-UNAM grants IG101320, IN111716-3, IN111419, IA102019, IN110621, IN110521; VIEP-BUAP; PIFI 2012, 2013, PROFOCIE 2014, 2015; the University of Wisconsin Alumni Research Foundation; the Institute of Geophysics, Planetary Physics, and Signatures at Los Alamos National Laboratory; Polish Science Centre grant, DEC-2017/27/B/ST9/02272; Coordinación de la Investigación Científica de la Universidad Michoacana; Royal Society - Newton Advanced Fellowship 180385; Generalitat Valenciana, grant CIDEGENT/2018/034; Chulalongkorn University's CUniverse (CUAASC) grant; Coordinación General Académica e Innovación (CGAI-UdeG), PRODEP-SEP UDG-CA-499; Institute of Cosmic Ray Research (ICRR), University of Tokyo, H.F. acknowledges support by NASA under award number 80GSFC21M0002. We also acknowledge the significant contributions over many years of Stefan Westerhoff, Gaurang Yodh and Arnulfo Zepeda Dominguez, all deceased members of the HAWC collaboration. Thanks to Scott Delay, Luciano Díaz and Eduardo Murrieta for technical support.

References

[1] A.U. Abeysekara et al., HAWC Collab., NIM A1052, (2023) 168253.
[2] R. Alfaro et al., HAWC Collab., Phys. Rev. D 96 (2017) 122001.
[3] S. Ostapchenko, Phys. Rev. D 83 (2011) 014018.
[4] A. U. Abeysekara et al., HAWC Collaboration, Astrophys. J. 881 (2019) 134.
[5] D. Heck et al., CORSIKA: A Monte Carlo Code to Simulate Extensive Air Showers, FZK Berichte 6019, Karlsruhe, Germany, 1998.
[6] A. D. Panov et al., ATIC-2 Collab., Bull. Russ. Acad. Sci. Phys. 73, No. 5 (2009) 564.
[7] H. S. Ahn et al., CREAM Collaboration, Astrophys. J. 707 (2009) 593.
[8] Y. S. Yoon et al., CREAM Collaboration, Astrophys. J. 728 (2011) 122.
[9] O. Adriani et al., PAMELA Collab., Science 332 (2011) 69.
[10] O. Adriani et al., PAMELA Collab., ApJ 791 (2014) 93.
[11] M. Aguilar et al., AMS Collab., Phys. Rev. Lett. 115 (2015) 211101.
[12] M. Aguilar et al., AMS Collab., Phys. Rev. Lett. 119 (2017) 251101.
[13] M. Aguilar et al., AMS Collab., Phys. Rev. Lett. 124 (2020) 211102.
[14] M. Aguilar et al., AMS Collab., Phys. Rev. Lett. 126 (2021) 041104.
[15] E. V. Atkin et al., NUCLEON Collaboration, Astron. Rep. 63 (2019) 66.
[16] O. Adriani et al., CALET Collab., Phys. Rev. Lett. 122 (2019) 181102.
[17] O. Adriani et al., (CALET Collaboration), Phys. Rev. Lett. 125 (2020) 251102.
[18] O. Adriani et al., (CALET Collaboration), Phys. Rev. Lett. 126 (2021) 241101.
[19] P. Brogi et al., CALET Collab., PoS ICRC2021 (2021) 101.
[20] Q. An et al., DAMPE Collab., Science Advances 5, No. 9 (2019) eaax3793.
[21] F. Alemanno et al., DAMPE Collab., PRL 126 (2021) 201102.
[22] T. Antoni et al., KASCADE Collab., Astrop. Phys. 24 (2005) 1.
[23] S. Agostinelli et al., NIMA 506 (2003) 250.
[24] R. Gold, An iterative unfoding method for response matrices, Report ANL-6984, Argonne National Laboratory, USA,1964.
[25] F. James, MINUIT - Function Minimization and Error Analysis Reference Manual, CERN Report number: CERN-D506.
[26] R. Brun and F. Rademakers, NIMA 389 (1997) 81.
[27] J. R. Hoerandel, Astropart. Phys. 19 (2003) 193.
[28] H. P. Dembinski et al., PoS(ICRC2017) 533.
[29] G. D'Agostini, A multidimensional unfolding method based on Bayes' theorem, NIMA 362, (1995) 487.
[30] T. K., Gaisser, Astropart. Phys. 35 (2012) 801.
[31] T. Pierog et al., Phys. Rev. C 92 (2015) 034906.
[32] O. Adriani et al., (CALET Collaboration), Phys. Rev. Lett. 129 (2022) 101102.
[33] Ivan De Mitri et al., DAMPE Collab., the 27th European Cosmic Ray Symposium (ECRS2022), Nijmegen, The Netherlands (2022).
[34] A. Albert et al., HAWC Collab., PRD 105, (2022) 063021.
[35] B. Bartoli et al., ARGO-YBJ Collaboration, PRD 92 (2015) 092005.
[36] Y. Takahashi et al., JACEE Collaboration, Nucl. Phys. B (Proc. Suppl.) 60 (1998) 83.
[37] V. I. Zatsepin et al., MUBEE Collaboration, Proc. of the 23rd ICRC (Calgary, Canada), Vol. 2, 1993, No. 13.
[38] Y. S. Yoon et al., CREAM Collaboration, Astrophys. J. 839 (2017) 5.
[39] G. H. Choi et al., ISS-CREAM Collab., PoS ICRC2021 (2021) 094.

Full Authors List: HAWC Collaboration

A. Albert[1], R. Alfaro[2], C. Alvarez[3], A. Andrés[4], J.C. Arteaga-Velázquez[5], D. Avila Rojas[2], H.A. Ayala Solares[6], R. Babu[7], E. Belmont-Moreno[2], K.S. Caballero-Mora[3], T. Capistrán[4], S. Yun-Cárcamo[8], A. Carramiñana[9], F. Carreón[4], U. Cotti[5], J. Cotzomi[26], S. Coutiño de León[10], E. De la Fuente[11], D. Depaoli[12], C. de León[5], R. Diaz Hernandez[9], J.C. Díaz-Vélez[11], B.L. Dingus[1], M. Durocher[1], M.A. DuVernois[10], K. Engel[8], C. Espinoza[2], K.L. Fan[8], K. Fang[10], N.I. Fraija[4], J.A. García-González[13], F. Garfias[4], H. Goksu[12], M.M. González[4], J.A. Goodman[8], S. Groetsch[7], J.P. Harding[1], S. Hernandez[2], I. Herzog[14], J. Hinton[12], D. Huang[7], F. Hueyotl-Zahuantitla[3], P. Hüntemeyer[7], A. Iriarte[4], V. Joshi[28], S. Kaufmann[15], D. Kieda[16], A. Lara[17], J. Lee[18], W.H. Lee[4], H. León Vargas[2], J. Linnemann[14], A.L. Longinotti[4], G. Luis-Raya[15], K. Malone[19], J. Martínez-Castro[20], J.A.J. Matthews[21], P. Miranda-Romagnoli[22], J. Montes[4], J.A. Morales-Soto[5], M. Mostafá[6], L. Nellen[23], M.U. Nisa[14], R. Noriega-Papaqui[22], L. Olivera-Nieto[12], N. Omodei[24], Y. Pérez Araujo[4], E.G. Pérez-Pérez[15], A. Pratts[2], C.D. Rho[25], D. Rosa-Gonzalez[9], E. Ruiz-Velasco[12], H. Salazar[26], D. Salazar-Gallegos[14], A. Sandoval[2], M. Schneider[8], G. Schwefer[12], J. Serna-Franco[2], A.J. Smith[8], Y. Son[18], R.W. Springer[16], O. Tibolla[15], K. Tollefson[14], I. Torres[9], R. Torres-Escobedo[27], R. Turner[7], F. Ureña-Mena[9], E. Varela[26], L. Villaseñor[26], X. Wang[7], I.J. Watson[18], F. Werner[12], K. Whitaker[6], E. Willox[8], H. Wu[10], H. Zhou[27]

[1]Physics Division, Los Alamos National Laboratory, Los Alamos, NM, USA, [2]Instituto de Física, Universidad Nacional Autónoma de México, Ciudad de México, México, [3]Universidad Autónoma de Chiapas, Tuxtla Gutiérrez, Chiapas, México, [4]Instituto de Astronomía, Universidad Nacional Autónoma de México, Ciudad de México, México, [5]Instituto de Física y Matemáticas, Universidad Michoacana de San Nicolás de Hidalgo, Morelia, Michoacán, México, [6]Department of Physics, Pennsylvania State University, University Park, PA, USA, [7]Department of Physics, Michigan Technological University, Houghton, MI, USA, [8]Department of Physics, University of Maryland, College Park, MD, USA, [9]Instituto Nacional de Astrofísica, Óptica y Electrónica, Tonantzintla, Puebla, México, [10]Department of Physics, University of Wisconsin-Madison, Madison, WI, USA, [11]CUCEI, CUCEA, Universidad de Guadalajara, Guadalajara, Jalisco, México, [12]Max-Planck Institute for Nuclear Physics, Heidelberg, Germany, [13]Tecnologico de Monterrey, Escuela de Ingeniería y Ciencias, Ave. Eugenio Garza Sada 2501, Monterrey, N.L., 64849, México, [14]Department of Physics and Astronomy, Michigan State University, East Lansing, MI, USA, [15]Universidad Politécnica de Pachuca, Pachuca, Hgo, México, [16]Department of Physics and Astronomy, University of Utah, Salt Lake City, UT, USA, [17]Instituto de Geofísica, Universidad Nacional Autónoma de México, Ciudad de México, México, [18]University of Seoul, Seoul, Rep. of Korea, [19]Space Science and Applications Group, Los Alamos National Laboratory, Los Alamos, NM USA [20]Centro de Investigación en Computación, Instituto Politécnico Nacional, Ciudad de México, México, [21]Department of Physics and Astronomy, University of New Mexico, Albuquerque, NM, USA, [22]Universidad Autónoma del Estado de Hidalgo, Pachuca, Hgo., México, [23]Instituto de Ciencias Nucleares, Universidad Nacional Autónoma de México, Ciudad de México, México, [24]Stanford University, Stanford, CA, USA, [25]Department of Physics, Sungkyunkwan University, Suwon, South Korea, [26]Facultad de Ciencias Físico Matemáticas, Benemérita Universidad Autónoma de Puebla, Puebla, México, [27]Tsung-Dao Lee Institute and School of Physics and Astronomy, Shanghai Jiao Tong University, Shanghai, China, [28]Erlangen Centre for Astroparticle Physics, Friedrich Alexander Universität, Erlangen, BY, Germany

PoS(ICRC2023)299